inter.noise 2014
MELBOURNE AUSTRALIA
16-19 NOVEMBER

Stochastic porous model of a bone-implant healing process using polynomial chaos expansion

Ji YANG[1]; Béatrice FAVERJON[1,2]; David DUREISSEIX[2]; Pascal SWIDER[3]; Nicole KESSISSOGLOU[1]

[1] School of Mechanical and Manufacturing Engineering, UNSW Australia, Sydney, NSW 2052, Australia

[2] Université de Lyon, CNRS, INSA-Lyon, LaMCoS UMR5259, F-69621, France

[3] IMFT UMR 5502 CNRS-INPT-Toulouse 3, France

ABSTRACT

Porous material is used in engineering and biomedical structures, where the solid phase is the frame of the material and dissipation effects occur in the pores of the material. This work proposes a stochastic model of porous material to predict the bone tissue healing process in the early period after the implantation surgery. The bone implant is assumed to be axisymmetric and the healing process is evaluated up to 8 weeks after the implantation, which is validated by the canine experiments. The porous dynamic model is coupled with biochemical equations to take into account the osteoblast cells migration and the growth factors diffusion. Using the polynomial chaos expansion method, the effects of uncertain biochemical factors on the distribution of the new-formed tissue around the bone implant are examined. Compared with Monte Carlo simulations, the stochastic model can obtain high accuracy with greatly improved computational cost. The spatial-temporal model presented here provides a tool to evaluate the highly complex implant healing process and the influences of different biochemical factors.

Keywords: Porous material, Stochastic model, Polynomial chaos expansion
I-INCE Classification of Subjects Number(s): 35.2.5

1. INTRODUCTION

The clinical longevity of an orthopedic implant is affected by its fixation to the surrounding bone (1, 2). The implant fixation quality is determined by the bone healing process in the early period after the implantation surgery, which is influenced by several mechanical and biochemical factors (3, 4, 5). The mechanical factors come from the nature of the bone. The bone structure is a porous medium and it consists of two parts, the solid phase is the bone matrix and the fluid phase is the marrow. The biochemical factors added to the mechanical behaviour are from the osteoblasts and growth factors, which proliferate and migrate in the marrow. The osteoblast cells promote bone formation and mineralization. The growth factors regulate cell proliferation and stimulate bone matrix formation (6).

A numerical model of a bone healing process involves both mechanical (7, 8, 9) and biochemical aspects (10, 11). Early models focused on the mechanical properties, which simplify the biochemical and time effects (10, 11). Models have been developed to examine the biological and transient behaviours of the cells and growth factors (12, 13, 14). The porous bone tissue was modelled as a convective-diffusive-reactive material (15, 16, 17) and was validated by experimental results (18, 19).

There are many uncertain parameters to consider in a numerical model of a bone implant which will affect the healing process. Models of uncertainty are generally based on either a parametric or non-parametric description of the uncertainty. The polynomial chaos expansion method is a parametric approach to describe uncertain parameters. The polynomial chaos expansion was first introduced as the homogeneous chaos (20) and is applied to examine systems with high levels of uncertainty (21). Using polynomial chaos expansion, the stochastic system equations are transformed to a set of deterministic equations using the Galerkin projection scheme. Compared with Monte Carlo simulations, polynomial chaos expansion can obtain the statistical characteristics of the results with greatly reduced computational cost.

This paper investigates the effects of uncertain biochemical factors on the bone-implant healing process using polynomial chaos expansion. The bone structure is modelled as a rigid porous material with a 1D (radial)

[1] ji.yang@unsw.edu.au

axisymmetric geometry, which supports an unloaded and axisymmetric implant. The mechano-biological model considers both the mechanical and biochemical equations to take into account the osteoblast cells migration and the growth factors diffusion. Results from the numerical model of the homogeneous healing of the bone implant are initially validated by experiment results from literature. Uncertainties within the healing process are then modelled using the polynomial chaos expansion method. The explicit finite difference scheme is combined with the polynomial chaos expansion method to solve the stochastic system equations. Results from the stochastic model are compared with Monte Carlo simulations.

2. POROUS MODEL FOR THE BONE IMPLANT

The diffusive–convective–reactive system equations of bone-implant healing have been developed based on porous material mechanics (7, 8, 9) and biomechanics (15).The bone structure consists of both solid and fluid phases, corresponding to the bone matrix and the marrow, respectively.

The coupled bone-implant healing process consists of the mineral deposit by osteoblast cells, the transport of growth factors by convection, the diffusion and migration of growth factors and osteoblast cells. For a rigid and axisymmetric bone implant, the mass conservations of each phase during the healing process are given in what follows (15)

$$\frac{\partial \phi^s}{\partial t} = \alpha^s (1-\phi^s)^2 C^c C^M \tag{1}$$

$$\mathbf{div}\mathbf{q}^{f/s} = -\alpha^s (1-\phi^s)^2 C^c C^M \tag{2}$$

$$\begin{aligned} \frac{\partial [(1-\phi^s)C^c]}{\partial t} =& \mathbf{div}\mathbf{q}^c + \alpha^c (1-\phi^s) C^c [N^{cc} - (1-\phi^s)C^c] \\ \text{with} \quad \mathbf{q}^c =& (1-\phi^s)(D^c \mathbf{grad} C^c - h^c \rho^s C^c \mathbf{grad}\phi^s - \chi^c C^c \mathbf{grad} C^M) \end{aligned} \tag{3}$$

$$\frac{\partial [(1-\phi^s)C^M]}{\partial t} = \mathbf{div}\mathbf{q}^M \quad \text{with} \quad \mathbf{q}^M = D^M (1-\phi^s)\mathbf{grad} C^M + C^M \mathbf{q}^{f/s} \tag{4}$$

α^s is the coefficient of osteoid synthesis, $\mathbf{q}^c$ is the cells flow rate, $\mathbf{q}^M$ is the growth factors flow rate, D^c is the coefficient of cell diffusion, h^c is the coefficient of haptotactic migration, ρ^s is the density of solid phase, χ^c is the coefficient of chemotactic migration, α^c is the coefficient of cell proliferation, N^{cc} is the inhibition level of cell proliferation, D^M is the coefficient of growth factor diffusion. The outputs of the numerical model are the solid fraction distribution in the bone structure ϕ^s, the relative fluid flow rate $\mathbf{q}^{f/s}$, the concentration of osteoblast cells C^C and the concentration of growth factors C^M.

$$C^c = \frac{n^c}{1-\phi^s} \tag{5}$$

$$C^M = \frac{n^M}{1-\phi^s} \tag{6}$$

where n^c is the amount of cells per bone element, n^M is the amount of growth factors per bone element.

3. STOCHASTIC MODEL

3.1 Polynomial chaos expansion

Using polynomial chaos expansion method, the stochastic system equations are transformed into deterministic equations as follows. The uncertain variables are initially projected onto a stochastic space spanned by a set of mutually orthogonal base polynomials Ψ_i, which are functions of a multi-dimensional random variable $\boldsymbol{\xi} = \{\xi_1, \xi_2, ..., \xi_n\}$. Every random variable has a corresponding random space $\xi_i \in \Omega_i (i = 1, 2, ..., n)$. The uncertain variable Y can then be expressed as (22)

$$Y(\boldsymbol{\xi}) = \sum_{i=0}^{\infty} Y_i \Psi_i(\boldsymbol{\xi}) \tag{7}$$

where Y_i are deterministic coefficients. The base polynomials Ψ_i are a set of multi-dimensional polynomials in terms of $\boldsymbol{\xi}$ with the following orthogonal relationship

$$\mathrm{E}[\Psi_i \Psi_j] = \delta_{ij} \mathrm{E}[\Psi_i^2] \tag{8}$$

δ_{ij} is the Kronecker delta and E represents the expected value in the probability space. Selection of the base polynomials Ψ_i depends on the probability density function of each random variable (23). Using the orthogonality relationship, the unknown coefficients Y_i can be determined by stochastic Galerkin projection.

3.2 Uncertain bone-implant healing

In this work, uncertainty in biochemical factors is examined. In what follows, the uncertain parameters α_s, h_c, χ_c are represented by truncated polynomial chaos expansion (PCE) using a limited number of base polynomials. Using N_α, N_h, N_χ to represent the number of base polynomials in the truncated PCE, the uncertain α^s, h^c, χ^c are respectively given by

$$\alpha^s(\boldsymbol{\xi}) = \sum_{p=0}^{N_\alpha} \alpha_p^s \Psi_p(\boldsymbol{\xi}) \quad , \quad h^c(\boldsymbol{\xi}) = \sum_{q=0}^{N_h} h_q^c \Psi_q(\boldsymbol{\xi}) \quad , \quad \chi^c(\boldsymbol{\xi}) = \sum_{r=0}^{N_\chi} \chi_r^c \Psi_r(\boldsymbol{\xi}) \tag{9}$$

The uncertain output parameters $\phi^s, q^{f/s}, C^c, C^M$ are then expressed by

$$\begin{aligned} \phi^s(\boldsymbol{\xi}) &= \sum_{i=0}^{N_\phi} \phi_i^s \Psi_i(\boldsymbol{\xi}) \quad , \quad \mathbf{q}^{f/s}(\boldsymbol{\xi}) = \sum_{j=0}^{N_q} \mathbf{q}_j^{f/s} \Psi_j(\boldsymbol{\xi}) \quad , \quad C^c(\boldsymbol{\xi}) = \sum_{k=0}^{N_c} C_k^c \Psi_k(\boldsymbol{\xi}) \\ C^M(\boldsymbol{\xi}) &= \sum_{l=0}^{N_M} C_l^M \Psi_l(\boldsymbol{\xi}) \end{aligned} \tag{10}$$

where N_ϕ, N_q, N_c, N_M are respectively the number of base polynomials in the truncated PCE for the output parameters. Substituting the expansion equations given by Eqs. (9) and (10) into Eqs. (1)-(4), multiplying by a base polynomial $\Psi_t(\boldsymbol{\xi})$ and then using Galerkin projection results in a set of deterministic equations. To solve the partial differential equations, the explicit finite difference scheme with variable time steps and upwinding is utilized .

4. NUMERICAL RESULTS

Figure 1 shows a schematic diagram of an axisymmetric bone implant investigated numerically in Ref. (2). An enlarged view of the implant shows the radius of the implant denoted by r_i, the radius of the drill hole denoted by r_d and the radius of the surrounding bone denoted by r_s. In a previous canine implant experiment (18, 19), the radii were measured as $r_i = 3.25$mm, $r_d = 4.1$mm and $r_s = 7$mm. The healing process is examined up to 8 weeks after the implantation surgery, where the implant is stable and axially unloaded.

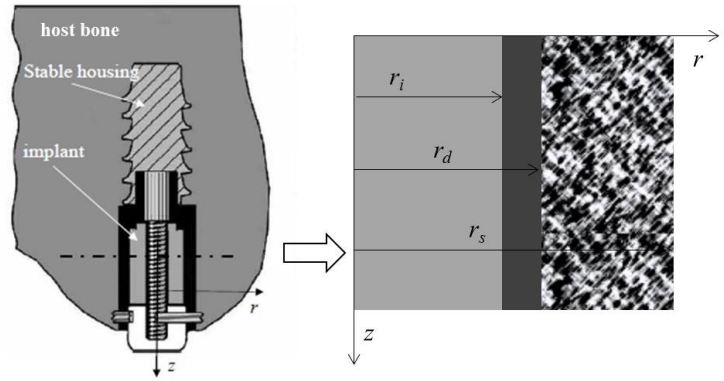

Figure 1 – Axisymmetric bone structure

The initial conditions of the numerical mechano-biological model used here are listed in Table 1. The fluid flow $\mathbf{q}^{f/s}$, cells flow $\mathbf{q}^c$ and growth factors flow $\mathbf{q}^M$ are zero at the implant surface boundary. The initial distribution of the solid fraction ϕ_0^s in the bone structure is modelled as

$$\phi_0^s = \frac{1}{2}(\phi_s^s + \phi_i^s) + \frac{1}{\pi}(\phi_s^s - \phi_i^s)\tan^{-1}\left[\frac{1}{\delta_d}(r - r_d)\right] \tag{11}$$

where ϕ_i^s, ϕ_s^s are the distribution of the solid fraction at implant surface and surrounding bone, $r \in [r_i, r_s]$ is the radius, δ_d is the transition region at the drill hole, δ_d, r_d depend on the surgery technique.

Table 1 – Initial conditions of the mechano-biological model

Parameter	New-formed tissue $[r_i, r_d]$	Surrounding bone $[r_d, r_s]$
ϕ^s[%]	6	10-60
$\mathbf{q}^{f/s}$[mm/s]	0	0
n^c[cell/mm^3]	[0,1000]	1000
C^M[ng/mm^3]	[0,0.3]	0

In the numerical model, the fixed and uncertain parameters are obtained from experiments and literature (2, 18, 19), as listed in Table 2.

Table 2 – Parameters of the mechano-biological model

Parameter	Value	Parameter	Value
δ_d[mm]	0.1	ϕ_s^s[%]	50
N^{cc}[cell/mm^3]	1000	C_i^M[ng/mm^3]	0.2
α^c[mm^3/(cell.s)]	1.9×10^{-10}	n_i^c[cell/mm^3]	1000
D^c[mm^2/s]	2.5×10^{-7}	α^s [mm^6/(cell.ng.s)]	$[1, 5]\times10^{-9}$
D^M[mm^2/s]	4.8×10^{-6}	h^c [mm^5/(s.kg)]	[0.04, 0.88]
ρ^s[kg/mm^3]	2.57×10^{-6}	χ^c [mm^5/(s.ng)]	$[1, 14.5]\times10^{-5}$

Experimental results reproduced from Refs. (15, 18, 19) are compared with results from the numerical model developed here, as shown in Fig. 2. For the deterministic numerical model in this work, the coefficient values within the range provided in Table 2 were chosen as follows: coefficient of osteoid synthesis α^s=3.25×10^{-9} mm^6/(cell.ng.s); coefficient of haptotactic migration h^c=0.7 mm^5/(s.kg); coefficient of chemotactic migration χ^c=7×10^{-5} mm^5/(s.ng). Figure 2 shows that the solid fraction distribution from the numerical model is in very close agreement with the experimental results. Compared with the surrounding original bone with a boundary value of ϕ_s^s=50% at radius r_s, the solid fraction distribution of the new-formed tissue in the gap between the implant and drill hole ($r \in [r_i, r_d]$) is relatively high. Two peak values for the solid fraction distribution occur around the implant surface ($r = r_i$, ϕ_i^s=75%) and the drill hole ($r = r_d$, ϕ_d^s=73%), which are close to each other. Outside the implant region ($r > r_d$), the solid fraction distribution decreases towards the boundary value ϕ_s^s.

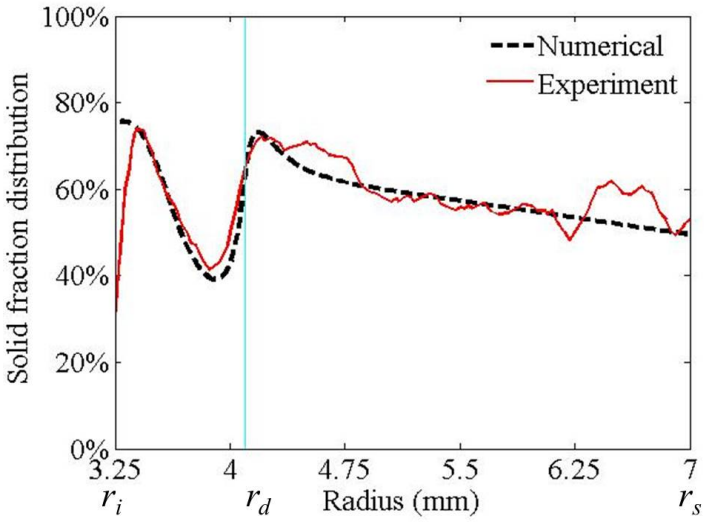

Figure 2 – Numerical and experimental results for the solid fraction distribution in the bone-implant structure

4.1 Uncertain coefficient of osteoid synthesis α^s

Variability in the coefficient of osteoid synthesis α^s is assumed to follow a uniform distribution within the range shown in Table 2, which is well represented by the 1st order Legendre PCE (N_α=1) (21). The uncertain

solid fraction distribution ϕ^s is represented by the 2nd order Legendre PCE (N_ϕ=2), which is accurate enough as shown in Fig. 3. The statistical moments of the uncertain output are obtained from the coefficients of the polynomial chaos expansion using the orthogonality of the base polynomials in Eq. (8). Upper and lower envelopes of the solid fraction distribution are constructed from the PCE expression. In each case, 50,000 Legendre polynomial samples are generated and substituted into the PCE expression to obtain the maximum and minimum values of ϕ^s. Results obtained using polynomial chaos expansion are compared with Monte Carlo (MC) simulations using 5000 samples. As shown in Fig. 3, both the mean and variance results can be well predicted by the Legendre PCE. Furthermore, the computational cost is significantly reduced using PCE as the 5000 MC simulations take 270 hours and the 2nd-order Legendre PCE takes 40 hours to compute. The coefficient of osteoid synthesis α^s influences the formation of bone in the whole structure ($r \in [r_i, r_s]$). The maximum variations show around the implant surface ($r = r_i$) and the drill hole ($r = r_d$). The synthesis of bone matrix is very active in the gap ($r \in [r_i, r_d]$) between the implant and drill hole, which also influences the solid fraction distribution in the surrounding bone.

4.2 Uncertain coefficient of haptotactic migration h^c

In this case, the variability comes from the uncertain coefficient of haptotactic migration h^c, which is assumed to follow a uniform distribution within the range shown in Table 2 and is represented by the 1st order Legendre PCE (N_h=1). As shown in Fig. 4, the coefficient of haptotactic migration h^c mainly influences the formation of bone in the gap ($r \in [r_i, r_d]$) between the implant and drill hole. Haptotactic flow is proportional to the gradient of solid fraction distribution (15). The maximum variations of the solid fraction distribution show in the gap and around the drill hole surface, which is attributed to the high gradient of solid fraction distribution in such regions.

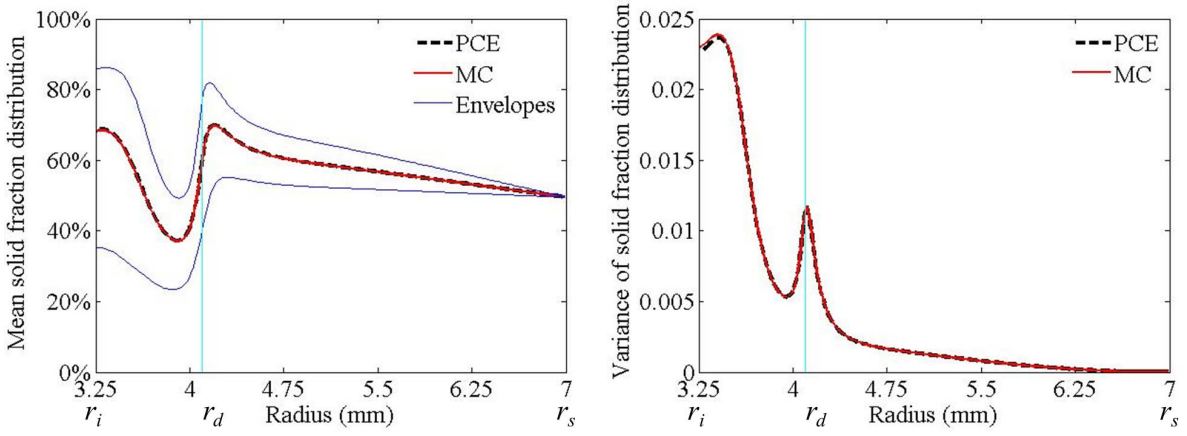

Figure 3 – Mean and variance of solid fraction distribution with uncertain coefficient of osteoid synthesis α^s

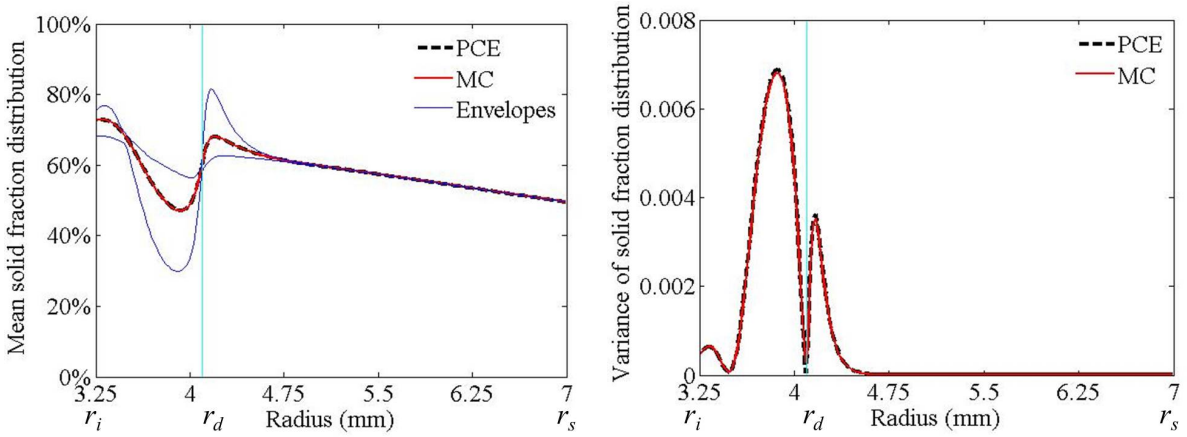

Figure 4 – Mean and variance of solid fraction distribution with uncertain coefficient of haptotactic migration h^c

4.3 Uncertain coefficient of chemotactic migration χ^c

Variability in the healing process is now generated by the uncertain coefficient of chemotactic migration χ^c, which is assumed to follow a uniform distribution within the range shown in Table 2 and is represented by the 1st order Legendre PCE (N_χ=1). As shown in Fig. 5, the coefficient of chemotactic migration χ^c influences the formation of bone in the gap ($r \in [r_i, r_d]$) between the implant and drill hole. Chemotactic flow is proportional to the gradient of growth factor concentration (15). The most significant variations of the solid fraction distribution occur around the implant surface ($r = r_i$), showing high gradient of growth factor concentration.

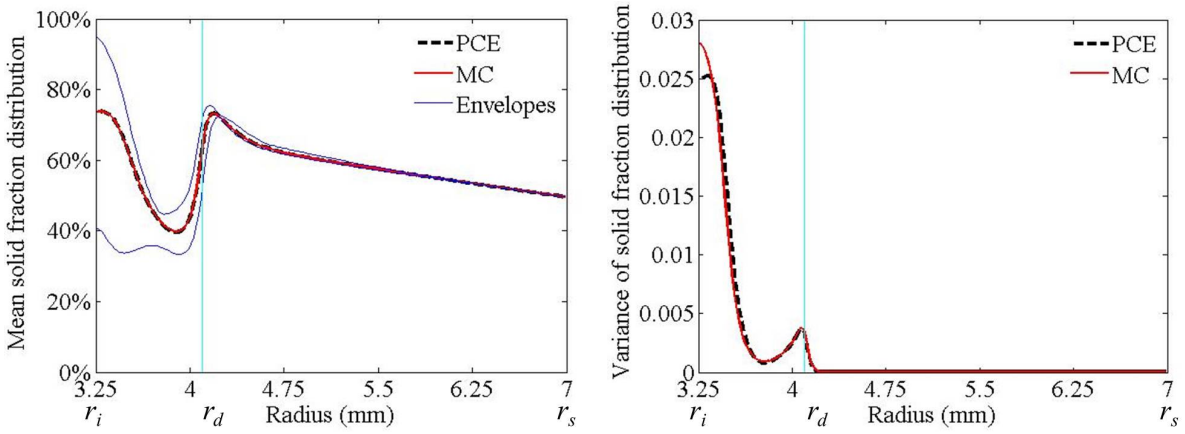

Figure 5 – Mean and variance of solid fraction distribution with uncertain coefficient of chemotactic migration χ^c

5. CONCLUSIONS

The bone-implant healing process in the early period after the surgery is crucial to the longevity of the implant, which is influenced by several uncertain parameters. This paper utilizes a mechano-biological model to predict the formation of bone structure up to 8 weeks after the implantation. The mechano-biological model is further combined with polynomial chaos expansion to examine the effects of uncertain biochemical factors. Compared with Monte Carlo simulations, the stochastic model is shown to obtain accurate results with much lower computational cost. For the single uncertain coefficient examined here, the computational time for this stochastic model is about 15% of that for the Monte Carlo simulations. Based on this stochastic model, the effects of osteoid synthesis, haptotactic and chemotactic migration are examined.

ACKNOWLEDGEMENT

The authors wish to thank J.E. Bechtold and K. Soballe for providing experimental results in collaboration with P. Swider.
Béatrice Faverjon gratefully acknowledges the French Education Ministry, University of Lyon, CNRS, INSA of Lyon and LabEx iMUST for the CRCT and the out mobility grant.

REFERENCES

1. Hahn M, Vogel M, Eckstein F, Pompesius-Kempa M, Delling G. Bone structure changes in hip joint endoprosthesis implantation over the course of many years. A quantitative study. Chirurgy. 1998;59(11):782–787.

2. Swider P, Ambard D, Guérin G, Søballe K, Bechtold JE. Sensitivity analysis of periprosthetic healing to cell migration, growth factor and post-operative gap using a mechanobiological model. Comput Method Biomec. 2011;14(9):763–771.

3. Morshed S, Bozic KJ, Ries MD, Malchau H, Colford JMJ. Comparison of cemented and uncemented fixation in total hip replacement: a meta-analysis. Acta Orthop. 2007;78(3):315–326.

4. Schwarz F, Herten M, Sager M, Wieland M, Dard M, Becker J. Histological and immunohistochemical analysis of initial and early osseous integration at chemically modified and conventional SLA titanium implants: preliminary results of a pilot study in dogs. Clin Oral Implan Res. 2007;18:481–488.

5. Colnot C, Romero DM, Huang S, Rahman J, Currey JA, Nancy A, et al. Molecular analysis of healing at a bone-implant interface. J Dent Res. 2007;86:862–867.

6. Conover CA. Skeletal Growth factors. Lippincott Williams Wilkins, Philadelphia; 2000.

7. Biot MA. Acoustics, Elasticity and Thermodynamics of Porous Media: Twenty one papers by M.A. Biot, in: I. Tolstoy (Ed.). Acoustical Society of America, New York; 1992.

8. Coussy O. Poromechanics. Wiley, Chichester, England; 2004.

9. Gorog S, R Panneton R, Atalla N. Mixed displacement-pressure formulation for acoustic anisotropic open porous media. J Appl Phys. 1997;82:4192–4196.

10. Carter DR, Blenman PR. Correlations between mechanical stress history and tissue differentiation in initial fracture healing. J Orthop Res. 1988;6:736–748.

11. Viceconti M, Muccini R, Bernakiewicz M, Baleani M, Cristofolini L. Large-sliding contact elements accurately predict levels of bone-implant micromotion relevant to osseointegration. J Biomech. 2000;33(12):1611–1618.

12. Bailon-Plaza A, Van der Meulen MC. A mathematical framework to study the effects of growth factor influences on fracture healing. J Theor Biol. 2001;212(2):191–209.

13. Geris L, Gerisch A, Sloten JV, Weiner R, Oosterwyck HV. Angiogenesis in bone fracture healing: a bioregulatory model. J Theor Biol. 2008;251(1):137–158.

14. Checa S, Prendergast PJ. A mechanobiological model for tissue differentiation that includes angiogenesis: a lattice-based modeling approach. Ann Biomed Eng. 2009;37:129–145.

15. Ambard D, Swider P. A predictive mechano-biological model of the bone-implant healing. Eur J Mech A/Solids. 2006;25:927–937.

16. Ambard D, Guérin G, Swider P. A reactive poroelastic model to predict the periprosthetic tissue healing. Eur J Comp Mech. 2009;18(1):131–143.

17. Guérin G, Ambard D, Swider P. Cells, growth factors and bioactive surface properties in a mechanobiological model of implant healing. J Biomech. 2009;42(15):2555–2561.

18. Søballe K, Hansen ES, B-Rasmussen H, Jorgensen PH, Bunger C. Tissue ingrowth into titanium and hydroxyapatite-coated implants during stable and unstable mechanical conditions. J Orthop Res. 1992;10(2):285–299.

19. Vestermark MT, Bechtold JE, Swider P, Søballe K. Mechanical interface conditions affect morphology and cellular activity of sclerotic bone rims forming around experimental loaded implants. J Orthop Res. 2004;22(3):647–652.

20. Wiener N. The homogeneous chaos. Am J Math. 1938;60:897–936.

21. Ghanem RG, Spanos PD. Stochastic Finite Elements: A Spectral Approach. Springer-Verlag, New York; 1991.

22. Xiu D, Karniadakis G. The Wiener–Askey polynomial chaos for stochastic differential equations. J Sci Comput. 2002;24(2):619–644.

23. Soize C, Ghanem R. Physical systems with random uncertainties: chaos representations with arbitrary probability measure. SIAM J SCI Comput. 2004;26(2):395–410.